# *Ab initio* intermolecular potential energy surface and second pressure virial coefficients of methane

Robert Hellmann, Eckard Bich, and Eckhard Vogel[a)]
*Institut für Chemie, Universität Rostock, Albert-Einstein-Straße 3a, D-18059 Rostock, Germany*

(Received 7 April 2008; accepted 29 April 2008; published online 3 June 2008)

A six-dimensional potential energy hypersurface (PES) for two interacting rigid methane molecules was determined from high-level quantum-mechanical *ab initio* computations. A total of 272 points for 17 different angular orientations on the PES were calculated utilizing the counterpoise-corrected supermolecular approach at the CCSD(T) level of theory with basis sets of aug-cc-pVTZ and aug-cc-pVQZ qualities. The calculated interaction energies were extrapolated to the complete basis set limit. An analytical site-site potential function with nine sites per methane molecule was fitted to the interaction energies. In addition, a semiempirical correction to the analytical potential function was introduced to take into account the effects of zero-point vibrations. This correction includes adjustments of the dispersion coefficients and of a single-parameter within the fit to the measured values of the second virial coefficient $B(T)$ at room temperature. Quantitative agreement was then obtained with the measured $B$ values over the whole temperature range of the measurements. The calculated $B$ values should definitely be more reliable at very low temperatures ($T<150$ K) than values extrapolated using the currently recommended equation of state. © *2008 American Institute of Physics*. [DOI: 10.1063/1.2932103]

## I. INTRODUCTION

Precise knowledge of the interaction potential between molecules is needed to calculate the thermophysical properties in the gas, liquid, or solid phases. In the case of a dilute pure gas, these properties can be determined from a molecule-molecule pair potential. Once the interaction potential is available, it is straightforward to compute the second pressure virial coefficient utilizing statistical mechanics. In addition, the transport and relaxation properties of dilute molecular gases are accessible by means of the kinetic theory of gases, which was recently extended to nonlinear molecules.[1] However, for dense gases, also liquid, and solid phases, nonadditive terms must be included in addition.

The interaction potential of the methane molecule pair was the subject of numerous studies over the past decades. In molecular simulations, the potential was very often approximated by a spherically symmetric Lennard-Jones type function in which the two adjustable parameters were fitted to experimental data. Furthermore, several *ab initio* calculations were performed, mostly concerned with the well depth at the global minimum or the distance dependence of the potential for that angular orientation providing the global minimum. To the best of our knowledge only two groups of researchers carried out *ab initio* studies in the last ten years in which multiple angular orientations were considered so that a complete anisotropic potential hypersurface could be derived.

In 1998, Tsuzuki *et al.*[2] calculated a total of 132 points on the potential energy hypersurface (PES) for 12 angular orientations at the MP3 level of theory. They used a 6-311G** basis set with additional diffuse polarization functions. A site-site potential energy function, with sites located at the carbon and hydrogen atoms, was then fitted to the calculated interaction energies. The resulting analytical potential function features a maximum well depth of 224 K. In 1999, Rowley and Pakkanen[3] calculated 146 energy points for 11 angular configurations at the MP2/6-311 +G(2*df*,2*pd*) level. They also derived a site-site potential function, with sites on the carbon and hydrogen atoms, characterized by a maximum well depth of only 168 K. In addition, Rowley and Pakkanen presented an improved potential function which was deduced by refitting to five selected points on the PES determined at the MP4 level with the aug-cc-pVTZ (Refs. 4 and 5) basis set. This procedure led to an increased well depth of 237 K. However, in 2006 Tsuzuki *et al.*[6] showed that the global minimum should actually be still deeper. They applied the very accurate CCSD(T) method,[7] employing basis sets up to cc-pVQZ,[4] and obtained global well depths of 252 and 263 K, depending on different procedures in extrapolating the interaction energies to the complete basis set (CBS) limit.

In order to obtain a more accurate methane-methane potential energy surface, a number of issues have to be taken into account. Thus, more reliable CBS estimates can be achieved by considering diffuse basis functions which generally improve the basis set convergence for weakly bound systems. Further, the influence of zero-point vibrations on the interaction potential should be incorporated. This effect is expected to be quite large, since the polarizability of methane is significantly higher when vibration is taken into consideration,[8,9] resulting in stronger attraction and therefore in a deeper well depth.

In the present paper, a new interaction potential energy

a)Electronic mail: eckhard.vogel@uni-rostock.de.

 

surface for methane has been determined using highly accurate coupled-cluster calculations with larger basis sets, performed for more angular orientations and more center of mass separations than in the previous studies. In addition, a more flexible analytical site-site potential model has been employed to minimize fitting errors. A semiempirical correction for zero-point vibrational effects has been included in the final analytical representation. The second pressure virial coefficient has been utilized to test the quality of the new potential.

In forthcoming papers, we will report on transport and relaxation property values of dilute methane gas computed with the new PES over a wide range of temperature. Accurate experimental values of transport properties at room temperature can be used as a further test of the validity of the potential energy surface. In addition, such calculations are of importance because viscosity and thermal conductivity are difficult to experimentally determine at very low and very high temperatures. Hence, we expect the theoretically computed values to be more accurate than the experimental data at extreme temperatures.

## II. QUANTUM CHEMICAL DETERMINATION AND ANALYTICAL REPRESENTATION OF THE $CH_4$–$CH_4$ POTENTIAL

Altogether 17 angular orientations with 16 center of mass separations, each between 2.5 and 8.0 Å, were chosen for the computations, resulting in a total of 272 interaction energies. These orientations are illustrated in Fig. 1. Due to the high symmetry of the methane molecule, this number of angular orientations should be adequate for the intended fit of a highly flexible analytical potential function to the calculated interaction energies.

The bond angles of $CH_4$ were established to give a regular tetrahedron. The length of the C–H bonds was fixed according to the experimental zero-point vibrationally averaged value of 1.099 Å.[10] This value is consistent with high-level *ab initio* computations of the bond length. An equilibrium bond length of 1.0859 Å was determined at the CCSD(T) level by Stanton[11] who employed large basis sets and performed an extrapolation to the CBS limit. Lee *et al.*[12] found that the increase in the bond length due to zero-point vibrations is 0.0131 Å at the CCSD(T)/cc-pVQZ level. The sum of both values yields again 1.099 Å.

Each interaction energy was calculated using the supermolecular approach including a full counterpoise correction[13] at the frozen-core CCSD(T) level with the aug-cc-pVTZ and aug-cc-pVQZ basis sets.[5] The correlation part of the CCSD(T) interaction energies, $V_{\mathrm{CCSD(T)corr}}$, obtained with these two basis sets was extrapolated to the CBS limit with the formula proposed by Halkier *et al.*,[14]

$$V^{XZ}_{\mathrm{CCSD(T)corr}} = V^{\mathrm{CBS}}_{\mathrm{CCSD(T)corr}} + \alpha X^{-3}. \tag{1}$$

The self-consistent-field interaction energies were not extrapolated and were taken from the aug-cc-pVQZ calculations.

An analytical site-site potential function was fitted to the extrapolated interaction energies. The positions of the sites

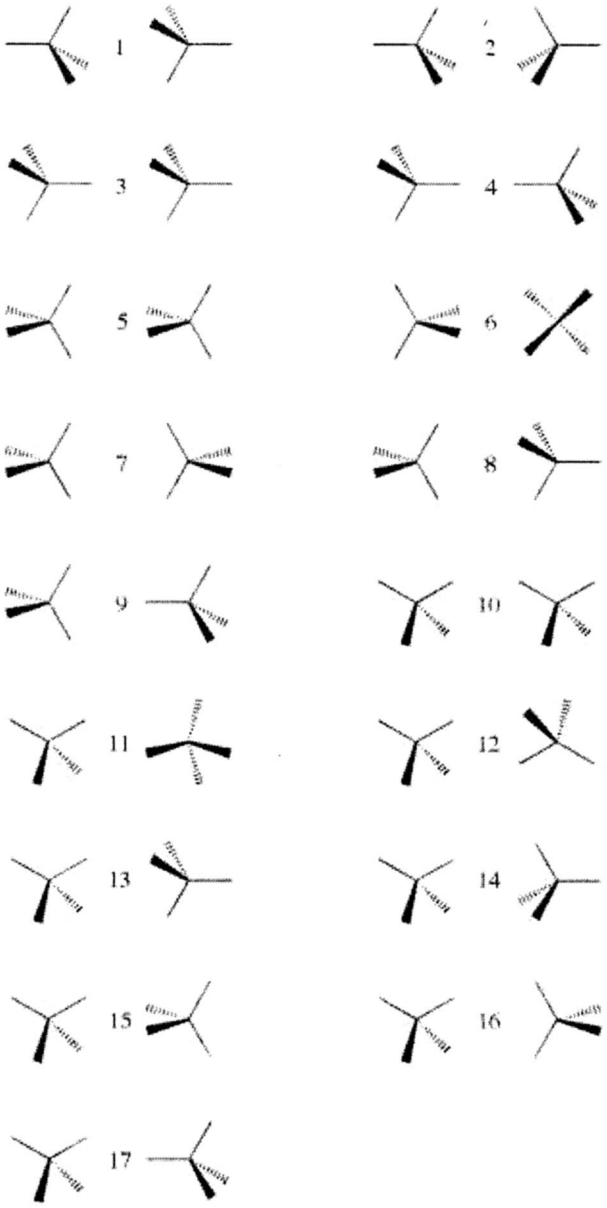


FIG. 1. Angular orientations of the methane molecules.

within the methane molecule are as follows: The $CH_4$ molecule is located at the center of a Cartesian coordinate system. One site denoted "C" corresponds to the carbon atom. Four sites denoted "H" are generated by scaling the Cartesian coordinates of the hydrogen atoms by 0.88, and four sites denoted "E" are obtained by scaling the Cartesian coordinates of the hydrogen atoms by −0.66. This procedure leads to a total of nine sites per molecule and enables an accurate fit of the *ab initio* values. The total potential is given as a function of the center of mass distance $R$ and of three Eulerian angles for each of the molecules A and B,

$$V(R,\vartheta_{\mathrm{A}},\vartheta_{\mathrm{B}},\psi_{\mathrm{A}},\psi_{\mathrm{B}},\varphi_{\mathrm{A}}-\varphi_{\mathrm{B}}) = \sum_{i=1}^{9}\sum_{j=1}^{9} V_{ij}[R_{ij}(R,\vartheta_{\mathrm{A}},\vartheta_{\mathrm{B}},\psi_{\mathrm{A}},\psi_{\mathrm{B}},\varphi_{\mathrm{A}}-\varphi_{\mathrm{B}})] \tag{2}$$

with

TABLE I. Comparison of the *ab initio* calculated values with the fitted ones for three angular orientations of the uncorrected $CH_4-CH_4$ potential.

| | Orientation 1 | | Orientation 4 | | Orientation 7 | |
|---|---|---|---|---|---|---|
| $R$ (Å) | *Ab initio* (K) | Fit (K) | *Ab initio* (K) | Fit (K) | *Ab initio* (K) | Fit (K) |
| 2.50 | 7843.67 | 8155.60 | 241671.0 | 110921.0 | 24103.2 | 23773.1 |
| 2.75 | 2727.14 | 2777.63 | 69568.3 | 52120.1 | 10053.8 | 9950.3 |
| 3.00 | 678.222 | 676.192 | 26117.1 | 23585.0 | 3894.51 | 3859.28 |
| 3.25 | −52.924 | −58.840 | 10597.0 | 10231.9 | 1303.41 | 1295.01 |
| 3.50 | −255.262 | −257.529 | 4251.28 | 4199.35 | 283.565 | 284.407 |
| 3.75 | −266.072 | −265.580 | 1582.87 | 1576.32 | −72.226 | −69.808 |
| 4.00 | −220.489 | −218.941 | 490.780 | 490.181 | −164.163 | −162.625 |
| 4.25 | −167.941 | −166.389 | 73.446 | 72.894 | −161.761 | −161.270 |
| 4.50 | −123.586 | −122.429 | −64.519 | −65.862 | −132.724 | −132.806 |
| 4.75 | −89.924 | −89.205 | −94.086 | −95.981 | −101.597 | −101.843 |
| 5.00 | −65.510 | −65.108 | −86.512 | −88.474 | −75.666 | −75.886 |
| 5.50 | −35.669 | −35.580 | −53.260 | −54.510 | −41.474 | −41.552 |
| 6.00 | −20.375 | −20.332 | −29.862 | −30.441 | −23.441 | −23.467 |
| 6.50 | −12.218 | −12.152 | −17.006 | −17.278 | −13.886 | −13.910 |
| 7.00 | −7.645 | −7.570 | −10.134 | −10.273 | −8.578 | −8.638 |
| 8.00 | −3.323 | −3.276 | −4.114 | −4.169 | −3.667 | −3.725 |

$$V_{ij}(R_{ij}) = A_{ij}\exp(-\alpha_{ij}R_{ij}) - f_6(R_{ij},b_{ij})\frac{C_{6ij}}{R_{ij}^6} - f_8(R_{ij},b_{ij})\frac{C_{8ij}}{R_{ij}^8} + \frac{q_i q_j}{R_{ij}}, \tag{3}$$

where $R_{ij}$ is the distance between site $i$ in molecule A and site $j$ in molecule B. The damping functions $f_6$ and $f_8$ were introduced by Tang and Toennies,[15]

$$f_n(R_{ij},b_{ij}) = 1 - \exp(-b_{ij}R_{ij})\sum_{k=0}^{n}\frac{(b_{ij}R_{ij})^k}{k!}. \tag{4}$$

The charges $q_i$ on the sites E were set to be zero, and the C and H charges were fitted to the octupole moment of the methane monomer calculated at the all-electron CCSD(T)/aug-cc-pV5Z level ($\Omega_{xyz}$=2.7231 a.u. in the standard orientation), with the sum of all charges being zero.

Fitting constraints concerning the dispersion coefficients were also applied. At large center of mass distances $R$ the site-site potential model gives isotropic dispersion interactions. This isotropy is consistent with the real long-range behavior of two uncharged tetrahedral molecules, where the interaction term with the slowest decay is the isotropic $C_6R^{-6}$ term.[16] Within the site-site potential model, the coefficient itself is given as $C_6=\Sigma_{i=1}^9\Sigma_{j=1}^9 C_{6ij}$ and was fixed to the value derived from supermolecular CCSD(T)/aug-cc-pVTZ calculations at asymptotic separations. These calculations were performed for distances between 20 and 30 Å for the angular orientation 7 in Fig. 1. The values of $V(R)R^6$ were calculated for each separation and then extrapolated to $R\rightarrow\infty$ resulting in $C_6^{\mathrm{sm}}$=853 300 K Å$^6$. This value is nearly independent of the basis set size and changes by less than 0.1% from aug-cc-pVDZ to aug-cc-pVTZ. A further constraint in the fitting process was that the isotropic part of the $C_8$ coefficient resulting from the site-site potential model as $C_{8,\mathrm{iso}}=\Sigma_{i=1}^9\Sigma_{j=1}^9 C_{8ij}$ should be equal to the value calculated by Fowler *et al.*[16] to be $C_{8,\mathrm{iso}}$=8 137 743 K Å$^8$.

The relative fitting errors are smaller than 2% for most calculated points on the PES. Significantly larger errors occur only at distances, where the potential goes through zero and in the highly repulsive region. The resulting analytical potential function has a maximum well depth of 273.9 K at $R$=3.633 Å for angular orientation 1 in Fig. 1. Table I shows the fitted potential curves and the respective *ab initio* data for three angular orientations.

To derive a correction for zero-point vibrational effects, the $C_6$ coefficient resulting from the supermolecular calculations $C_6^{\mathrm{sm}}$=853 300 K Å$^6$ was compared with the value inferred from spectral data by Thomas and Meath[17] as $C_6^{\mathrm{exp}}$=898 647 K Å$^6$, which includes zero-point vibrational effects. The difference between these two values is denoted as $\Delta C_6=C_6^{\mathrm{exp}}-C_6^{\mathrm{sm}}$. Assuming that the relative effect of the zero-point vibrations would be similar for the isotropic part of $C_8$, an estimation of $\Delta C_{8,\mathrm{iso}}$ follows from

$$\Delta C_{8,\mathrm{iso}} = C_{8,\mathrm{iso}}\frac{\Delta C_6}{C_6^{\mathrm{sm}}}. \tag{5}$$

The corrected potential is then given as the sum of the uncorrected potential and an isotropic correction term,

$$V_{\mathrm{corr}}(R,\vartheta_A,\vartheta_B,\psi_A,\psi_B,\varphi_A-\varphi_B) = V_{\mathrm{uncorr}}(R,\vartheta_A,\vartheta_B,\psi_A,\psi_B,\varphi_A-\varphi_B) + \Delta V_{\mathrm{corr}}(R) \tag{6}$$

with

$$\Delta V_{\mathrm{corr}}(R) = -f_6(R,b_{\mathrm{corr}})\frac{\Delta C_6}{R^6} - f_8(R,b_{\mathrm{corr}})\frac{\Delta C_{8,\mathrm{iso}}}{R^8}. \tag{7}$$

Here, the parameter $b_{\mathrm{corr}}$ is still adjustable and was chosen so that the second pressure virial coefficient at room temperature computed with the corrected potential agrees well with

TABLE II. Potential parameters. The number in parenthesis is the power of 10.

| | $A$ (K) | $\alpha$ (Å$^{-1}$) | $b$ (Å$^{-1}$) | $C_6$ (K Å$^6$) | $C_8$ (K Å$^8$) |
|---|---|---|---|---|---|
| C–C | 0.262 373 610(7) | 0.168 784 21(1) | 0.168 275 675(1) | 0.112 317 356(7) | −0.120 939 119(9) |
| C–H | 0.265 413 949(7) | 0.288 272 19(1) | 0.288 261 054(1) | −0.139 633 537(7) | 0.385 078 060(8) |
| H–H | 0.241 399 203(6) | 0.359 175 61(1) | 0.384 703 188(1) | 0.294 147 230(6) | −0.264 781 786(7) |
| C–E | −0.271 732 286(6) | 0.164 907 47(1) | 0.155 011 960(1) | 0.127 844 394(7) | 0.174 762 764(7) |
| H–E | −0.749 715 218(5) | 0.205 930 86(1) | 0.266 424 603(1) | 0.169 329 268(6) | −0.810 401 688(7) |
| E–E | 0.123 654 939(6) | 0.214 516 41(1) | 0.304 993 944(1) | −0.590 727 146(6) | 0.679 543 866(7) |

| | |
|---|---|
| $\Delta C_6$ | 0.45347(5) K Å$^6$ |
| $\Delta C_{8,\mathrm{iso}}$ | 0.432463(6) K Å$^8$ |
| $b_{\mathrm{corr}}$ | 0.177(1) Å$^{-1}$ |
| $q_{\mathrm{H}}$ | 0.94753(2) (K Å)$^{1/2}$ |
| $q_{\mathrm{C}}$ | −0.379012(3) (K Å)$^{1/2}$ |

the most accurate experimental data (see Sec. IV). The correction increases the maximum well depth to 286.0 K at 3.624 Å associated with orientation 1. The parameters of the corrected intermolecular potential hypersurface are given in Table II, whereas $V_{\mathrm{corr}}$ is shown in Fig. 2 as a function of the center of mass separation $R$ for eight of the chosen angular orientations. The minimum well depth of only 99.8 K at 4.776 Å is represented by orientation 4 in Fig. 2, which distinctly illustrates the anisotropy of the potential, but also the "hard-sphere" size of the interaction.

All *ab initio* calculations were performed with the Mainz–Austin–Budapest version of ACES II (Ref. 18) and with GAUSSIAN 03.[19]

## III. QUANTUM-MECHANICAL CALCULATION OF THE SECOND PRESSURE VIRIAL COEFFICIENT

The second pressure virial coefficients $B(T)$ can be very accurately measured, particularly around room temperature. Hence, such data provide a valuable test for the intermolecular pair potential of the molecules when compared with values computed using statistical mechanics. Such calculations cannot be performed reliably classically when the temperatures are low and when atoms or molecules with small masses or small moments of inertia are considered. At very low temperatures and for light spherically symmetric atoms a fully quantum mechanical treatment of the elastic scattering using phase shifts and including quantum statistical effects is needed, whereas the treatment of nonspherical systems requires the solution of the coupled-channel scattering problem.[20,21]

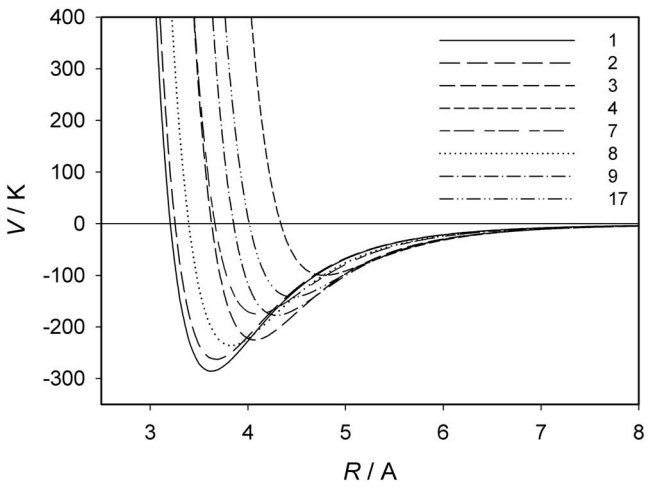


FIG. 2. The corrected intermolecular potential $V$ as a function of the mass separation $R$ for eight angular orientations (numbering according to Fig. 1).

In this paper, two alternative ways were used to calculate the second virial coefficient of methane as a function of temperature $T$. In the first variant it is assumed that a sufficiently accurate calculation of the second virial coefficients should be possible by adding quantum corrections, significant in the Boltzmann limit, to the classical contribution. Pack[21] derived an expression for the first quantum correction to the second virial coefficient, valid for the interaction of like and unlike rigid-rotor molecules, such as diatomics, spherical tops, and symmetric tops, but excluding asymmetric tops. Using angular momentum theory, Wormer[22] recently developed a formalism, correct at the level of the first-order quantum correction, for the second virial coefficient of a gas consisting of identical interacting rigid-rotor molecules of any symmetry, including asymmetric tops. Based on these papers, explicit formulae for the first quantum corrections are given here for the computation of the second virial coefficient of rigid asymmetric top molecules. Then, they are applied to methane treated as rigid spherical tops under the assumption that vibrations are negligibly excited.

The second virial coefficient $B(T)$ is related to the one-particle and two-particle partition functions $Q_1$ and $Q_2$ according to[23]

$$B(T) = -\frac{N_A V}{2}\left[\frac{2Q_2(T) - Q_1^2(T)}{Q_1^2(T)}\right]. \tag{8}$$

Here, $N_A$ is Avogadro's number and $V$ is the volume. The classical contribution to $B(T)$ for a gas consisting of interacting asymmetric top molecules A and B is given as

$$B_{\mathrm{cl}}(T) = -\frac{N_A}{128V\pi^4}\int \cdots \int [\mathrm{e}^{-\beta V(\mathbf{R}_A,\Omega_A;\mathbf{R}_B,\Omega_B)} - 1] \times d\mathbf{R}_A d\Omega_A d\mathbf{R}_B d\Omega_B, \tag{9}$$

where

$$\beta = 1/(k_B T), \quad d\mathbf{R}_i = R_i^2 dR_i \sin\theta d\theta d\phi, \tag{10}$$

$$d\Omega_i = \sin\vartheta_i d\vartheta_i d\varphi_i d\psi_i. \tag{11}$$

$V(\mathbf{R}_A, \Omega_A; \mathbf{R}_B, \Omega_B)$ is the intermolecular pair potential and $k_B$ is Boltzmann's constant. $\mathbf{R}_i$ locates the center of mass of molecule $i$ in a space-fixed coordinate system, whereas $\Omega_i$ are the rotational coordinates. $\theta$ and $\phi$ are the polar angles, whereas $\varphi_i$, $\vartheta_i$, and $\psi_i$ are the Eulerian angles.

After transformation to the center of mass of the molecule pair and to relative coordinates

$$\mathbf{R} = \mathbf{R}_B - \mathbf{R}_A, \tag{12}$$

$$V(\mathbf{R}_A, \Omega_A; \mathbf{R}_B, \Omega_B) = V(\mathbf{R}, \Omega_A, \Omega_B), \tag{13}$$

the classical contribution is

$$B_{cl}(T) = -\frac{N_A}{128\pi^4} \int \cdots \int [e^{-\beta V(\mathbf{R}, \Omega_A, \Omega_B)} - 1] \times d\mathbf{R} d\Omega_A d\Omega_B. \tag{14}$$

The computation of $B_{cl}(T)$ can be performed under the assumption that molecule A is fixed in the space-fixed coordinate system and that the integration over the Eulerian angles of molecule A leads to

$$B_{cl}(T) = -\frac{N_A}{16\pi^2} \int_0^{2\pi} \int_0^{2\pi} \int_0^{\pi} \int_0^{2\pi} \int_0^{\pi} \int_0^{\infty} \times [e^{-\beta V(R, \theta, \phi, \vartheta_B, \psi_B, \varphi_B)} - 1] \times R^2 dR \sin\theta d\theta d\phi \sin\vartheta_B d\vartheta_B d\psi_B d\varphi_B. \tag{15}$$

Here, molecule B moves around molecule A (integration over $R$, $\theta$, and $\phi$) and rotates about its axes (integration over $\vartheta_B$, $\psi_B$, and $\varphi_B$).

After transforming again to center of mass-relative coordinates and using the fact that the derivatives of the intermolecular pair potential $V(\mathbf{R}, \Omega_A, \Omega_B)$ vanish with respect to the center of mass coordinates, the first-order quantum correction to the second virial coefficient can be formulated as

$$B_{qm}^{(1)}(T) = -\frac{N_A}{128\pi^4} \int \cdots \int e^{-\beta V} \frac{\beta^2}{12} \hat{H}^0 V d\mathbf{R} d\Omega_A d\Omega_B, \tag{16}$$

$$\hat{H}^0 = \hat{H}_{tr,\mu} + \hat{H}_{rot,A} + \hat{H}_{rot,B}. \tag{17}$$

$\hat{H}^0$ is the translation-rotation Hamiltonian operator in which the translational part $\hat{H}_{tr,\mu}$ is that for the hypothetical particle with the reduced mass $\mu$ of the pair of molecules and is given as

$$\hat{H}_{tr,\mu} = -\frac{\hbar^2}{2\mu} \nabla_{tr,\mu} \nabla_{tr,\mu}. \tag{18}$$

The rotational part of the Hamiltonian operator $\hat{H}_{rot,i}$ of a molecule $i$ can be written as

$$\hat{H}_{rot,i} = -\frac{\hbar^2}{2} \nabla_{rot,i} \nabla_{rot,i}. \tag{19}$$

The computation of $B_{qm}^{(1)}(T)$ is again carried out under the assumption that molecule A is fixed in the space-fixed coordinate system and that the integration over the Eulerian angles of molecule A can be performed analytically,

$$B_{qm}^{(1)}(T) = -\frac{N_A}{16\pi^2} \frac{\beta^2}{12} \int \cdots \int e^{-\beta V} \times (\hat{H}_{tr,\mu} + \hat{H}_{rot,A} + \hat{H}_{rot,B}) V d\mathbf{R} d\Omega_B. \tag{20}$$

It is convenient to take into account that upon integration by parts generally for any coordinates $\mathbf{x}_1$ and $\mathbf{x}_2$

$$\int e^{-\beta V} \nabla_i \nabla_i \beta V d\mathbf{x}_1 d\mathbf{x}_2 = \int e^{-\beta V} (\nabla_i \beta V)^2 d\mathbf{x}_1 d\mathbf{x}_2. \tag{21}$$

The translational part of the first-order quantum correction to the second virial coefficient related to identical molecules with the molecular mass $m$ and the reduced mass $\mu = m/2$ is

$$B_{tr}^{(1)}(T) = \frac{N_A}{16\pi^2} \frac{\hbar^2 \beta}{24\mu} \int_0^{2\pi} \int_0^{2\pi} \int_0^{\pi} \int_0^{2\pi} \int_0^{\pi} \int_0^{\infty} \times e^{-\beta V} [\nabla_{tr,\mu} \beta V]^2 R^2 \times dR \sin\theta d\theta d\phi \sin\vartheta_B d\vartheta_B d\psi_B d\varphi_B, \tag{22}$$

with

$$(\nabla_{tr,\mu} \beta V)^2 = \left(\frac{\partial \beta V}{\partial R}\right)^2 + \frac{1}{R^2}\left(\frac{\partial \beta V}{\partial \theta}\right)^2 + \frac{1}{R^2 \sin^2\theta}\left(\frac{\partial \beta V}{\partial \phi}\right)^2. \tag{23}$$

The rotational part of the first-order quantum correction to the second virial coefficient for two identical asymmetric top molecules with $\hat{H}_{rot,A} = \hat{H}_{rot,B}$ can be formulated as

$$B_{rot}^{(1)}(T) = \frac{N_A}{16\pi^2} \frac{\hbar^2 \beta}{12} \int \cdots \int e^{-\beta V} [\nabla_{rot,B} \beta V]^2 d\mathbf{R} d\Omega_B, \tag{24}$$

$$= \frac{N_A}{16\pi^2} \frac{\hbar^2 \beta}{12} \int_0^{2\pi} \int_0^{2\pi} \int_0^{\pi} \int_0^{2\pi} \int_0^{\pi} \int_0^{\infty} \times e^{-\beta V} \left(\frac{J_{x,B}^2}{I_{x,B}} + \frac{J_{y,B}^2}{I_{y,B}} + \frac{J_{z,B}^2}{I_{z,B}}\right) \times R^2 dR \sin\theta d\theta d\phi \sin\vartheta_B d\vartheta_B d\psi_B d\varphi_B. \tag{25}$$

$$J_{x,B} = \sin\psi_B \left(\frac{\partial \beta V}{\partial \vartheta_B}\right) - \frac{\cos\psi_B}{\sin\vartheta_B}\left(\frac{\partial \beta V}{\partial \varphi_B}\right) + \frac{\cos\psi_B \cos\vartheta_B}{\sin\vartheta_B}\left(\frac{\partial \beta V}{\partial \psi_B}\right), \tag{26}$$

$$J_{y,\mathrm{B}} = \cos\psi_{\mathrm{B}}\left(\frac{\partial\beta V}{\partial\vartheta_{\mathrm{B}}}\right) + \frac{\sin\psi_{\mathrm{B}}}{\sin\vartheta_{\mathrm{B}}}\left(\frac{\partial\beta V}{\partial\varphi_{\mathrm{B}}}\right) - \frac{\sin\psi_{\mathrm{B}}\cos\vartheta_{\mathrm{B}}}{\sin\vartheta_{\mathrm{B}}}\left(\frac{\partial\beta V}{\partial\psi_{\mathrm{B}}}\right), \tag{27}$$

$$J_{z,\mathrm{B}} = \left(\frac{\partial\beta V}{\partial\psi_{\mathrm{B}}}\right). \tag{28}$$

Here, $I_{x,\mathrm{B}}$, $I_{y,\mathrm{B}}$, and $I_{z,\mathrm{B}}$ are the Cartesian components of the moment of inertia of molecule B, whereas $J_{x,\mathrm{B}}$, $J_{y,\mathrm{B}}$, and $J_{z,\mathrm{B}}$ are the components of the body-fixed angular momentum operator formulated with Eulerian angles according to the $y$ convention.[24]

In the case of spherical-top molecules such as methane with $I=I_x=I_y=I_z$ the rotational first-order quantum correction follows from

$$B^{(1)}_{\mathrm{rot,sphtop}}(T) = \frac{N_A}{16\pi^2}\frac{\hbar^2\beta}{12I}\int_0^{2\pi}\int_0^{2\pi}\int_0^{\pi}\int_0^{2\pi}\int_0^{\pi}\int_0^{\infty} \times \mathrm{e}^{-\beta V}(J^2_{x,\mathrm{B}} + J^2_{y,\mathrm{B}} + J^2_{z,\mathrm{B}}) \times R^2 dR \sin\theta d\theta d\phi \sin\vartheta_{\mathrm{B}} d\vartheta_{\mathrm{B}} d\psi_{\mathrm{B}} d\varphi_{\mathrm{B}}. \tag{29}$$

Schenter[25] used an exact quantum-mechanical expression for the second virial coefficient based on Feynman path integration[26,27] in which the potential $V$ in the classical expression [Eq. (14)] is replaced by an effective potential $V_{\mathrm{eff}}$ which accounts for the quantum effects. Further, Schenter discussed in this paper a semiclassical approximation for $V_{\mathrm{eff}}$, originally proposed by Takahashi and Imada,[28] to improve the first-order quantum correction given in Eq. (20). Schenter showed that the results for the approximation by Takahashi and Imada are in excellent agreement with his exact calculations in the case of $H_2O$ and $D_2O$ except for the lowest temperatures. In our second variant, we used this semiclassical form for the effective intermolecular potential to calculate the second virial coefficient of methane. The procedure can be formulated as

$$B_{\mathrm{path}}(T) = -\frac{N_A}{128\pi^4}\int\cdots\int[\mathrm{e}^{-\beta V_{\mathrm{eff}}} - 1]d\mathbf{R}d\Omega_{\mathrm{A}}d\Omega_{\mathrm{B}}, \tag{30}$$

with

$$V_{\mathrm{eff}} = V(\mathbf{R},\Omega_{\mathrm{A}},\Omega_{\mathrm{B}}) + \frac{\beta}{12}\hat{H}_0 V(\mathbf{R},\Omega_{\mathrm{A}},\Omega_{\mathrm{B}}). \tag{31}$$

Here, $\beta\hat{H}_0 V$ can be replaced by

$$\beta\hat{H}_0 V \simeq \frac{\hbar^2}{2\mu}\left[\left(\frac{\partial\beta V}{\partial R}\right)^2 + \frac{1}{R^2}\left(\frac{\partial\beta V}{\partial\theta}\right)^2 + \frac{1}{R^2\sin^2\theta}\left(\frac{\partial\beta V}{\partial\phi}\right)^2\right] + \hbar^2\left[\left(\frac{J^2_{x,\mathrm{B}}}{I_{x,\mathrm{B}}} + \frac{J^2_{y,\mathrm{B}}}{I_{y,\mathrm{B}}} + \frac{J^2_{z,\mathrm{B}}}{I_{z,\mathrm{B}}}\right)\right]. \tag{32}$$

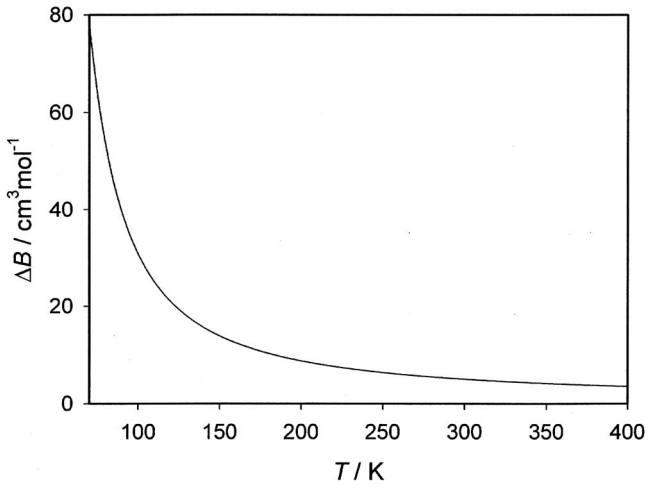


FIG. 3. Effect $\Delta B$ according to the approximated path-integration method as a function of temperature resulting from the fit of calculated second virial coefficients to the best experimental data at room temperature[30] in order to adjust $b_{\mathrm{corr}}$ of the corrected intermolecular potential energy surface for $CH_4$. $\Delta B = B_{\mathrm{path,uncorrected}} - B_{\mathrm{path,corrected}}$.

The computations of the values for the second virial coefficients are characterized by numerical uncertainties which are smaller than $\pm 0.01$ cm$^3$ mol$^{-1}$.

## IV. ADJUSTMENT OF THE INTERMOLECULAR POTENTIAL ENERGY SURFACE AND COMPARISON WITH EXPERIMENTAL DATA OF THE SECOND VIRIAL COEFFICIENT

A critical compilation of experimental data for the second pressure virial coefficient of methane was reported by Wagner and de Reuck.[29] The second virial data were included by these authors in the optimization of the equation of state (EOS) for methane, using a reduced Helmholtz energy. According to their evaluation, the experimental data by Kleinrahm *et al.*[30] are considered to be the most accurate at ambient temperature. These data were chosen to adjust the parameter $b_{\mathrm{corr}}$ in Eqs. (6) and (7), as already mentioned in Sec. II. In this procedure the quantum-mechanical calculation of the second virial coefficient was performed using the approximated path-integration method, see Eqs. (30)–(32).

The influence on the second virial coefficient of the change from the uncorrected to the corrected intermolecular potential hypersurface is shown in Fig. 3 as a function of temperature. The figure makes evident that the correction is strongly temperature dependent, but it is relatively small (5.1 cm$^3$ mol$^{-1}$) at room temperature. Figure 4 illustrates the temperature dependence of the quantum correction $B_{\mathrm{qm}}$ calculated by the approximated path-integration procedure and by summing of the translational and rotational first-order quantum corrections $B^{(1)}_{\mathrm{tr}}$ and $B^{(1)}_{\mathrm{rot,sphtop}}$ [see Eq. (22) and (29)]. The figure indicates that, in general, the quantum correction to the second virial coefficient is rapidly increasing as temperature decreases. Furthermore, the quantum correction resulting from the approximated path-integration method is smaller than the sum of the first-order quantum corrections

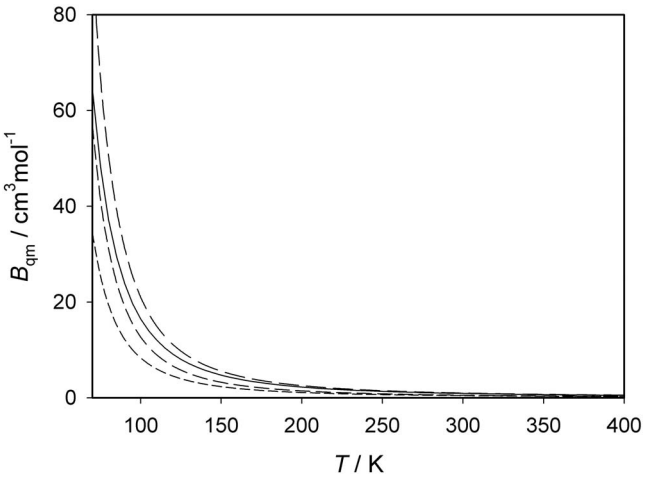


FIG. 4. Quantum corrections $B_{qm}$ calculated for the new corrected intermolecular potential energy surface for $CH_4$ as a function of temperature: - - - - - translational part of the first-order quantum correction $B_{tr}^{(1)}$, – – – – rotational part of the first-order quantum correction for spherical-top molecules $B_{rot,sphtop}^{(1)}$, — — — sum of the translational and rotational parts of the first-order quantum correction for spherical-top molecules $B_{tr}^{(1)}+B_{rot,sphtop}^{(1)}$, and ——— quantum correction according to the approximated path-integration method calculated as difference $B_{qm}=B_{path}-B_{cl}$.

$B_{tr}^{(1)}+B_{rot,sphtop}^{(1)}$. This is in agreement with the experience that the second-order quantum correction for monatomic gases is negative.[31]

The comparison with experimental second virial coefficients, shown as deviations $(B_{exp}-B_{cal})$ in Fig. 5, is restricted to the best available data. The comparison of experimental second virial coefficients with the values calculated theoretically depends on density measurements. These must be determined from pressure and volume measurements using an EOS which employs higher virial coefficients. These coefficients are in turn dependent on the second virial coefficient of interest. In our comparison only second virial coefficients are considered so that we rely on the assessment by Wagner and de Reuck.[29] However, unlike Wagner and de Reuck, who assigned some second pressure virial coefficients determined from speed of sound measurements via acoustic second virial coefficients[47,48] to their group 1 data, we did not consider them as proper primary data of highest accuracy. Hence only the data by Esper *et al.*,[45] derived from acoustic second virial coefficients, were included in the comparison, but not classified as group 1 data.

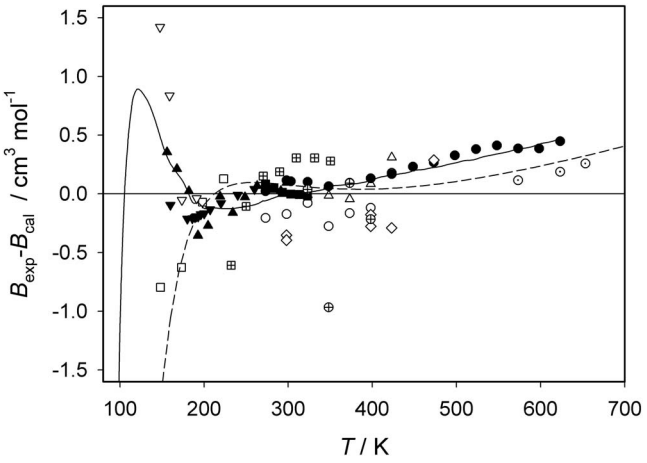


FIG. 5. Deviations of experimental and experimentally based second pressure virial coefficients from values calculated with the new corrected intermolecular potential energy surface using the path-integration method for $CH_4$ in a large temperature range. Experimental data: ● Douslin and Harrison (Ref. 32), ▲ Roe (Ref. 33), ■ Kleinrahm *et al.* (Ref. 30), ▼ Händel *et al.* (Ref. 34), ○ Michels and Nederbragt (Ref. 35), reevaluated by Pompe and Spurling (Ref. 36), △ Schamp, Jr. *et al.* (Ref. 37), □ Brewer (Ref. 38) (one additional value with $\Delta B=-2.64$ cm$^3$ mol$^{-1}$ at 123 K), ▽ Pope *et al.* (Ref. 39) (two additional values with $\Delta B=+6.14$ and $+1.96$ cm$^3$ mol$^{-1}$ at 127 and 137 K), ◇ Katayama *et al.* (Ref. 40), Ohgaki *et al.* (Refs. 41 and 42), ⊕ Mallu and Viswanath (Ref. 43), ⊙ Abdulagatov *et al.* (Ref. 44), and ⊞ Esper *et al.* (Ref. 45). Experimentally based data: —— values from the equation of state by Wagner and de Reuck (Ref. 29) and - - - - values calculated by means of an isotropic potential (fitted to experimental data) by Zarkova *et al.* (Ref. 46).

The remaining group 1 data are characterized in Fig. 5 by filled symbols and are discussed first. After adjusting the parameter $b_{corr}$ at room temperature, the values calculated for the new intermolecular potential of methane are in excellent agreement within $\pm 0.08$ cm$^3$ mol$^{-1}$ in the full temperature range from 273 to 323 K with the experimental data by Kleinrahm *et al.*,[30] determined with an absolute uncertainty of $\pm 0.15$ cm$^3$ mol$^{-1}$ using the two-sinker method based on the buoyancy principle. The figure makes evident that the calculated values are also consistent in the complete temperature range of 160–260 K with the results of experiments, performed by Händel *et al.*[34] applying the two-sinker method with an absolute uncertainty of $\pm 0.3$ cm$^3$ mol$^{-1}$. The analogous statement is valid for the Burnett-method measurements carried out and evaluated by Roe[33] to gain second pressure virial coefficients. The calculated values perfectly agree again within the claimed uncertainty of $\pm 0.6$ cm$^3$ mol$^{-1}$ at 156 K to $\pm 0.1$ cm$^3$ mol$^{-1}$ at 291 K. Whereas these low-temperature data show random scatter around the calculated values, the high-temperature data by Douslin *et al.*[32] between 273 and 623 K with an uncertainty of $\pm 0.2$ cm$^3$ mol$^{-1}$, derived from isochoric compressibility measurements, systematically differ by up to $+0.5$ cm$^3$ mol$^{-1}$ from the calculated values.

These calculations cast some doubt on the reliability of the second virial coefficients obtained by Wagner and de Reuck[29] from their optimization process for the equation of state of methane. Since the data by Händel *et al.*[34] were not used in generating the EOS, they systematically deviate by up to $-0.4$ cm$^3$ mol$^{-1}$ from the equation according to figure 1.17 of Ref. 29. On the contrary, the data of Douslin *et al.*[32] show virtually no differences to the EOS, because they were used to determine the equation. This also becomes obvious from our Fig. 5, in which the second virial coefficients corresponding to the EOS of methane are presented as a solid curve. The differences of our calculated values from this curve at higher temperatures could possibly originate from a deficient consideration of the vibrational modes of motion. On the other hand, the measurements by Douslin *et al.* could possibly be influenced by small systematic errors.

The other experimental second virial coefficients included in the comparison in Fig. 5 partly deviate in a systematic manner from the curve connected with the EOS, but also from the basic line corresponding to the values theoretically calculated for the new intermolecular potential. This is

TABLE III. Second pressure virial coefficients of methane for the new intermolecular potential.

| $T$ (K) | $B_{path}$ ($cm^3\ mol^{-1}$) | $B_{cl}$ ($cm^3\ mol^{-1}$) | $T$ (K) | $B_{path}$ ($cm^3\ mol^{-1}$) | $B_{cl}$ ($cm^3\ mol^{-1}$) | $T$ (K) | $B_{path}$ ($cm^3\ mol^{-1}$) | $B_{cl}$ ($cm^3\ mol^{-1}$) |
|---|---|---|---|---|---|---|---|---|
| 70.00 | −847.10 | −911.46 | 220.00 | −86.22 | −88.02 | 470.00 | −4.81 | −5.19 |
| 75.00 | −720.69 | −768.93 | 230.00 | −78.59 | −80.21 | 480.00 | −3.56 | −3.92 |
| 80.00 | −623.43 | −660.69 | 240.00 | −71.75 | −73.22 | 490.00 | −2.37 | −2.72 |
| 85.00 | −546.64 | −576.15 | 250.00 | −65.59 | −66.94 | 500.00 | −1.23 | −1.57 |
| 90.00 | −484.69 | −508.56 | 260.00 | −60.02 | −61.25 | 510.00 | −0.15 | 0.48 |
| 95.00 | −433.79 | −453.45 | 270.00 | −54.95 | −56.09 | 520.00 | 0.88 | 0.57 |
| 100.00 | −391.31 | −407.76 | 273.15 | −53.45 | −54.56 | 530.00 | 1.87 | 1.56 |
| 105.00 | −355.37 | −369.32 | 280.00 | −50.33 | −51.38 | 540.00 | 2.82 | 2.52 |
| 110.00 | −324.61 | −336.59 | 290.00 | −46.09 | −47.07 | 550.00 | 3.72 | 3.43 |
| 115.00 | −298.02 | −308.40 | 293.15 | −44.83 | −45.79 | 560.00 | 4.59 | 4.31 |
| 120.00 | −274.81 | −283.90 | 298.15 | −42.90 | −43.82 | 570.00 | 5.42 | 5.15 |
| 125.00 | −254.39 | −262.42 | 300.00 | −42.20 | −43.11 | 580.00 | 6.22 | 5.95 |
| 130.00 | −236.31 | −243.44 | 310.00 | −38.61 | −39.46 | 590.00 | 6.98 | 6.73 |
| 135.00 | −220.18 | −226.57 | 320.00 | −35.29 | −36.08 | 600.00 | 7.72 | 7.47 |
| 140.00 | −205.71 | −211.46 | 330.00 | −32.21 | −32.96 | 610.00 | 8.42 | 8.18 |
| 145.00 | −192.67 | −197.88 | 340.00 | −29.34 | −30.05 | 620.00 | 9.10 | 8.87 |
| 150.00 | −180.85 | −185.59 | 350.00 | −26.67 | −27.34 | 650.00 | 11.00 | 10.78 |
| 155.00 | −170.10 | −174.43 | 360.00 | −24.18 | −24.81 | 700.00 | 13.73 | 13.53 |
| 160.00 | −160.27 | −164.25 | 370.00 | −21.85 | −22.45 | 750.00 | 16.03 | 15.86 |
| 165.00 | −151.26 | −154.93 | 380.00 | −19.66 | −20.23 | 800.00 | 17.99 | 17.83 |
| 170.00 | −142.97 | −146.36 | 390.00 | −17.61 | −18.15 | 850.00 | 19.67 | 19.53 |
| 175.00 | −135.32 | −138.46 | 400.00 | −15.67 | −16.19 | 900.00 | 21.13 | 21.00 |
| 180.00 | −128.24 | −131.16 | 410.00 | −13.85 | −14.34 | 950.00 | 22.40 | 22.28 |
| 185.00 | −121.66 | −124.39 | 420.00 | −12.13 | −12.60 | 1000.00 | 23.51 | 23.41 |
| 190.00 | −115.54 | −118.09 | 430.00 | −10.50 | −10.95 | 1100.00 | 25.37 | 25.27 |
| 195.00 | −109.83 | −112.23 | 440.00 | −8.97 | −9.40 | 1200.00 | 26.83 | 26.75 |
| 200.00 | −104.49 | −106.74 | 450.00 | −7.51 | −7.92 | ⋯ | ⋯ | ⋯ |
| 210.00 | −94.79 | −96.80 | 460.00 | −6.12 | −6.52 | ⋯ | ⋯ | ⋯ |

particularly evident for the low-temperature data by Brewer[38] and Pope *et al.*,[39] each characterized by deviations distinctly larger than the claimed uncertainties of $\pm 1.3\ cm^3\ mol^{-1}$ at 123 K to $\pm 0.4\ cm^3\ mol^{-1}$ at 223 K for the data by Brewer and of $\pm 0.7\ cm^3\ mol^{-1}$ at 126 K to $\pm 0.2\ cm^3\ mol^{-1}$ at 191 K for the data by Pope *et al.* These measurements are not suitable to judge the quality of the new intermolecular potential surface of methane.

Figure 5 also shows a comparison with values recommended as reference data by Zarkova *et al.*[46] In the case of methane the basis for these values is an isotropic three-parameter Lennard-Jones-$(n-6)$ potential obtained from a multiproperty fit to experimental data for the second pressure and acoustic virial coefficients as well as for viscosity and self-diffusion at low density. It is to point out that the increasing deviations of the values by Zarkova *et al.* from our values toward lower temperature are due to the inclusion of low-temperature $B$ data of Byrne *et al.*[49] into their fit. However, these data were assessed by Wagner and de Reuck only as group 3 data and hence not considered for the EOS. Further these data are characterized by increasing differences to our calculated values with the maximum of $-10.2\ cm^3\ mol^{-1}$ at 111 K.

Ultimately, we are convinced that the calculations of this paper are more reliable than the EOS for low temperatures down to 70 K, for which no experimental second virial coefficients of high accuracy were available below 150 K. If we assume that vibrational excitations have only a negligible impact on the second virial coefficient we expect further that the computations for higher temperatures are also reliable. Values for the second pressure virial coefficient of methane recommended on the basis of the intermolecular potential of this work are given in Table III for the temperature range of 70–1200 K.

## V. SUMMARY AND CONCLUSIONS

A new intermolecular potential energy surface for two rigid methane molecules was determined from quantum-mechanical *ab initio* calculations. Altogether 272 interaction energies on the PES were determined at the CCSD(T) level of theory. Utilizing large basis sets up to aug-cc-pVQZ, the interaction energies were extrapolated to the CBS limit. A highly accurate site-site potential function was fitted to the calculated interaction energies, and in addition a physically reasonable correction for zero-point vibrational effects was established by a single-parameter fit to the most accurate experimental value of the second pressure virial coefficient at room temperature. The resulting potential shows a high anisotropy. It is characterized by a significantly greater well depth, 286 K, than previous interaction potentials.

The quality of the new potential was tested by computing the second pressure virial coefficient. For this purpose, explicit formulae were derived to calculate quantum correc-

tions to the classical second virial coefficient in terms of Euler angle coordinates for rigid asymmetric tops, which includes methane as the special case of a spherical top. The agreement with the most accurate experimental data is very good over a wide range of temperatures. A main contribution of this paper consists in providing accurate values down to very low temperatures where experimental data of high quality are unavailable. In a series of forthcoming papers, the new potential will be employed for the calculation of transport and relaxation properties of dilute methane gas over a wide range of temperatures.

## ACKNOWLEDGMENTS

The authors would like to acknowledge inspiring discussions with A. S. Dickinson (Newcastle University) and V. Vesovic (Imperial College London). This work was supported by the Deutsche Forschungsgemeinschaft (German Research Foundation) under Contract No. VO 499/14-1.

[1] A. S. Dickinson, R. Hellmann, E. Bich, and E. Vogel, Phys. Chem. Chem. Phys. **9**, 2836 (2007).
[2] S. Tsuzuki, T. Uchimaru, and K. Tanabe, Chem. Phys. Lett. **287**, 202 (1998).
[3] R. L. Rowley and T. Pakkanen, J. Chem. Phys. **110**, 3368 (1999).
[4] T. H. Dunning, Jr., J. Chem. Phys. **90**, 1007 (1989).
[5] D. E. Woon and T. H. Dunning, Jr., J. Chem. Phys. **100**, 2975 (1994).
[6] S. Tsuzuki, K. Honda, T. Uchimaru, and M. Mikami, J. Chem. Phys. **124**, 114304 (2006).
[7] K. Raghavachari, G. W. Trucks, J. A. Pople, and M. Head-Gordon, Chem. Phys. Lett. **157**, 479 (1989).
[8] A. J. Russell and M. A. Spackman, Mol. Phys. **84**, 1239 (1995).
[9] D. M. Bishop, F. L. Gu, and S. M. Cybulski, J. Chem. Phys. **109**, 8407 (1998).
[10] M. Nakata and K. Kuchitsu, J. Chem. Soc. Jpn., 1446 (1986).
[11] J. F. Stanton, Mol. Phys. **97**, 841 (1999).
[12] T. J. Lee, J. M. L. Martin, and P. R. Taylor, J. Chem. Phys. **102**, 254 (1995).
[13] S. F. Boys and F. Bernardi, Mol. Phys. **19**, 553 (1970).
[14] A. Halkier, T. Helgaker, P. Jørgensen, W. Klopper, H. Koch, J. Olsen, and A. K. Wilson, Chem. Phys. Lett. **286**, 243 (1998).
[15] K. T. Tang and J. P. Toennies, J. Chem. Phys. **80**, 3726 (1984).
[16] P. W. Fowler, P. Lazzeretti, and R. Zanasi, Mol. Phys. **68**, 853 (1989).
[17] G. F. Thomas and W. J. Meath, Mol. Phys. **34**, 113 (1977).
[18] J. F. Stanton, J. Gauss, J. D. Watts, P. G. Szalay, and R. J. Bartlett, with contributions from A. A. Auer, D. B. Bernholdt, O. Christiansen, M. E. Harding, M. Heckert, O. Heun, C. Huber, D. Jonsson, J. Jusélius, W. J. Lauderdale, T. Metzroth, C. Michauk, D. R. Price, K. Ruud, F. Schiffmann, A. Tajti, M. E. Varner, J. Vázquez, and the following integral packages: MOLECULE (J. Almlöf and P. R. Taylor), PROPS (P. R. Taylor), and ABACUS (T. Helgaker, H. J. Aa. Jensen, P. Jørgensen, and J. Olsen). See also J. F. Stanton, J. Gauss, J. D. Watts, W. J. Lauderdale, and R. J. Bartlett, Int. J. Quantum Chem., Symp. **26**, 879 (1992). For current version, see http://www.aces2.de
[19] M. J. Frisch, G. W. Trucks, H. B. Schlegel *et al.*, GAUSSIAN 03, Revision D.01, Gaussian, Inc., Wallingford, CT, 2004.
[20] L. Monchick, Chem. Phys. Lett. **24**, 91 (1974).
[21] R. T. Pack, J. Chem. Phys. **78**, 7217 (1983).
[22] P. E. S. Wormer, J. Chem. Phys. **122**, 184301 (2005).
[23] D. A. McQuarrie, *Statistical Mechanics* (Harper and Row, New York, 1976).
[24] C. G. Gray and K. E. Gubbins, *Theory of Molecular Fluids, Volume I: Fundamentals* (Clarendon, Oxford, 1984).
[25] G. K. Schenter, J. Chem. Phys. **117**, 6573 (2002).
[26] R. P. Feynman and A. R. Hibbs, *Quantum Mechanics and Path Integrals* (McGraw-Hill, New York, 1965).
[27] H. Kleinert, *Path Integrals in Quantum Mechanics Statistics and Polymer Physics* (World Scientific, New Jersey, 1995).
[28] M. Takahashi and M. Imada, J. Phys. Soc. Jpn. **53**, 3765 (1984).
[29] W. Wagner and K. M. de Reuck, *Methane. International Thermodynamic Tables of the Fluid State-13*, International Union of Pure and Applied Chemistry (Blackwell, Oxford, 1996).
[30] R. Kleinrahm, W. Duschek, W. Wagner, and M. Jaeschke, J. Chem. Thermodyn. **20**, 621 (1988).
[31] E. Bich, R. Hellmann, and E. Vogel, "*Ab initio* potential energy curve for the neon atom pair and thermophysical properties for the dilute neon gas. II. Thermophysical properties for low-density neon," Mol. Phys. (in press).
[32] D. R. Douslin, R. H. Harrison, R. T. Moore, and J. P. McCullough, J. Chem. Eng. Data **9**, 358 (1964).
[33] D. R. Roe, *Thermodynamic Properties of Gases and Gas Mixtures at Low Temperatures and High Pressures*, Ph.D. Thesis, University of London, 1972.
[34] G. Händel, R. Kleinrahm, and W. Wagner, J. Chem. Thermodyn. **24**, 685 (1992).
[35] A. Michels and G. W. Nederbragt, Physica (Amsterdam) **3**, 569 (1936).
[36] A. Pompe and T. H. Spurling, "Virial Coefficients for Gaseous Hydrocarbons," CSIRO Australia Div. Appl. Organic Chem. Tech. Paper No. 1, (1974).
[37] H. W. Schamp, Jr., E. A. Mason, A. C. B. Richardson, and A. Altman, Phys. Fluids **1**, 329 (1958).
[38] J. Brewer, "Determination of Mixed Virial Coefficients," U.S. Clearinghouse Fed. Sci. Tech. Information No. AD 663448, 1967.
[39] G. A. Pope, P. S. Chappelear, and R. Kobayashi, J. Chem. Phys. **59**, 423 (1973).
[40] T. Katayama, K. Ohgaki, and H. Ohmori, J. Chem. Eng. Jpn. **13**, 257 (1980).
[41] K. Ohgaki, Y. Nakamura, H. Ariyasu, and T. Katayama, J. Chem. Eng. Jpn. **15**, 85 (1982).
[42] K. Ohgaki, N. Sakai, Y. Kano, and T. Katayama, J. Chem. Eng. Jpn. **17**, 545 (1984).
[43] B. V. Mallu and D. S. Viswanath, J. Chem. Thermodyn. **22**, 997 (1990).
[44] I. M. Abdulagatov, A. R. Bazaev, and A. E. Ramazanova, J. Chem. Thermodyn. **25**, 249 (1993).
[45] G. Esper, W. Lemming, W. Beckermann, and F. Kohler, Fluid Phase Equilib. **105**, 173 (1995).
[46] L. Zarkova, U. Hohm, and M. Damyanova, J. Phys. Chem. Ref. Data **35**, 1331 (2006).
[47] W. Lemming, Fortschr.-Ber. VDI, Reihe 6 **19**, Nr. 32 (1989) (in German).
[48] W. Beckermann, Fortschr.-Ber. VDI, Reihe 6 **19**, Nr. 67 (1993) (in German).
[49] M. A. Byrne, M. R. Jones, and L. A. K. Staveley, Trans. Faraday Soc. **64**, 1747 (1968).